Am J Physiol Cell Physiol 330: C794–C806, 2026.
First published February 21, 2026; doi:10.1152/ajpcell.00312.2025

american physiological society

AMERICAN JOURNAL OF PHYSIOLOGY
CELL PHYSIOLOGY

RESEARCH ARTICLE

Placental small extracellular vesicles as modulators of bisphenol A-induced oxidative stress and mitochondrial activation in human astrocytoma cells (U-373 MG)

Serena Nencini,[1] Alice Pifferi,[1] Sofia Passaponti,[2] Filiberto Maria Severi,[3] Caterina Bocchi,[3] Silvia Canaletti,[3] Roberta Romagnoli,[1] Laura Cresti,[1] Leonardo Ermini,[1] and Francesca Ietta[1]

[1]*Department of Life Sciences, University of Siena, Siena, Italy;* [2]*Department of Medicine, Surgery and Neuroscience, University of Siena, Siena, Italy; and* [3]*Department of Molecular and Developmental Medicine, Division of Prenatal Diagnosis and Obstetrics, University of Siena, Siena, Italy*

Abstract

Astrocytes play a crucial role in maintaining central nervous system homeostasis, supporting neuronal function and regulating oxidative stress. The placenta, through the secretion of small extracellular vesicles (sEVs), facilitates communication between the maternal and fetal environments, potentially mitigating external stressors. Bisphenol A (BPA), an endocrine disruptor, has been implicated in oxidative stress and mitochondrial dysfunction, particularly in the developing brain. However, the mechanisms by which placental sEVs influence astrocyte responses to BPA remain unclear. This study investigates the effects of BPA on astrocyte oxidative stress and mitochondrial activity and explores how placental sEVs modulate these responses. Human glioblastoma astrocytoma (U-373 MG) cells were exposed to environmentally relevant concentrations of BPA (10 nM), with or without placental sEVs isolated from human term placental explants. Reactive oxygen species (ROS) levels, mitochondrial activation, and antioxidant enzyme expression (SOD1, GCLC, and GSTA) were assessed. Direct BPA exposure increased astrocyte ROS levels and mitochondrial activation, indicative of oxidative stress. Placental sEVs were rapidly internalized by astrocytes and counteracted BPA-induced ROS accumulation, restoring mitochondrial homeostasis. Notably, sEVs from BPA-exposed placental explants were more efficiently incorporated into astrocytes, suggesting an adaptive response. sEVs treatment also upregulated antioxidant enzyme expression and reduced inflammatory cytokine markers (CCL2 and IL-1β), indicating a potential protective mechanism. These findings suggest that placental sEVs play a critical role in modulating astrocyte responses to oxidative stress and mitochondrial dysfunction. The ability of sEVs to restore redox homeostasis highlights their potential physiological function in fetal neuroprotection against environmental stressors.

NEW & NOTEWORTHY The study demonstrates that BPA induces oxidative stress and mitochondrial dysfunction in human astrocytes. It introduces a novel role of sEVs in counteracting these effects by reducing ROS, restoring mitochondrial activity, and upregulating antioxidant enzymes. Notably, sEVs from BPA-exposed placental explants were more efficiently incorporated into astrocytes, suggesting an adaptive protective mechanism. These findings highlight a potential fetal neuroprotective role of placental sEVs against environmental stressors.

astrocytes; BPA; oxidative stress; placental extracellular vesicles

INTRODUCTION

Environmental and occupational exposure to endocrine-disrupting chemicals poses a significant threat to human health (1–3). Bisphenol A (BPA), a chemical produced by the condensation of two phenolic groups, is a key monomer in polycarbonate plastics and epoxy resins. It is widely used in consumer products such as water bottles, food and beverage can linings, and thermal paper. Due to its pervasive use, BPA has become a major global chemical pollutant (4–6). High temperatures can cause BPA to leach into food and beverages or disperse into the environment, exposing people to this endocrine disruptor through inhalation, ingestion, and skin contact. As a result, BPA is commonly found in various tissues and body fluids, including saliva, urine, and sweat (7).

BPA can affect the body through various pathways (8) and is known to exhibit endocrine-disrupting effects due to its estrogen-like properties. It interacts with multiple receptors, including estrogen receptors (ERs) and androgen receptors (ARs), acting as an agonist for ERs and antagonist for ARs (9). In addition, BPA can bind thyroid hormone receptors, interfering with normal thyroid function and disrupting the development and function of various organs (10, 11).

Correspondence: F. Ietta (ietta@unisi.it).
Submitted 8 April 2025 / Revised 30 April 2025 / Accepted 11 February 2026

Exposure to BPA has been linked to changes in glucose homeostasis, potentially contributing to the development of type 2 diabetes mellitus in pregnant women (12, 13); lipid accumulation and adipogenesis, increasing the risk of obesity (14); altered reproductive function in both males and females (15); and an elevated risk of cancers, particularly breast and prostate cancer (16). Moreover, BPA exposure has been associated with the onset of cardiovascular diseases (8). Furthermore, bisphenols interfere with vascular function by stimulating nitric oxide and endothelial nitric oxide synthase production (17).

BPA is able to penetrate the blood-brain barrier and thus acts at the level of the central nervous system (CNS), where it influences both development and inflammatory processes in the brain (18, 19). There is a need to study the effects of prenatal exposure to chemicals released from everyday objects, especially those that may interfere with the endocrine system of the unborn child. In fact, the early stages of human development are very susceptible to even the slightest hormonal perturbations, which can even lead to adverse birth outcomes or future diseases (20). Recent data have revealed that BPA not only crosses the placental barrier but also accumulates in fetal serum and amniotic fluid, exposing the fetus to higher concentrations than those found in maternal fluids (21, 22). In rodents in particular, fetal exposure to BPA affects neurodevelopmental processes, whereas exposure during childhood or adolescence can damage CNS cells, leading to functional changes and cell death (19). The mechanisms underlying BPA effects appear to be mediated by an induction of reactive oxygen species (ROS), which may contribute significantly to the diverse and pleiotropic effects observed following BPA exposure (19, 23).

Oxidative stress occurs when intracellular homeostasis is disrupted due to metabolic disturbances or toxic insults, leading to an imbalance between pro-oxidant and antioxidant substances. This results in increased ROS formation, damage to lipids and proteins, and cellular consequences such as impaired DNA repair and mitochondrial dysfunction. Under normal physiological conditions, the antioxidant system counteracts ROS generation through cellular antioxidant enzymes and powerful antioxidant molecules, both macro- and micro-sized (24). At the physiological level, ROS function as signaling molecules that regulate cellular processes, including proliferation, survival, cell death, differentiation, cell signaling, and the production of inflammation-related factors (25). High levels of oxidative stress are commonly observed in the brains of patients with autism and neurodevelopmental disorders. An overload of ROS has been shown to impair mitochondrial function, activate apoptotic cascades, and contribute to increased neuroinflammation by causing redox imbalances that alter cellular signaling (26). A toxicological approach focusing on the direct effects of stressors on the fetus has been used to link prenatal stress with pathological outcomes in the brain. However, proper embryo and fetal development depend on a healthy intrauterine environment and the functioning of the placenta, which provides oxygen, nutrients, and signaling molecules (such as steroids, cytokines, glycoproteins, and extracellular vesicles) to the developing fetus (27). In particular, small extracellular vesicles (sEVs) play a crucial role in transmitting signals to target cells, modulating processes such as inflammation, apoptosis, angiogenesis, and embryonic growth and development (28).

Gestational exposure to single and/or multiple environmental stressors can significantly disrupt the homeostasis between the mother, placenta, and fetus (29). Recent research suggests that exposure to environmental chemicals during pregnancy may alter the placenta's secretory and metabolic processes, as well as the expression profile of sEVs (30–32). In this study, we explored the direct and placental-mediated effects (via sEVs) of BPA on the oxidative status and mitochondrial activation of astrocytes, the most abundant glial cells in the CNS, that provide functional protection to neurons and contribute to maintaining the correct homeostasis of the CNS.

MATERIALS AND METHODS

A graphical representation summarizing the different experimental procedures, including *1*) placental explant culture, BPA exposure, and sEVs isolation and characterization; and *2*) astrocytoma cell treatments (direct BPA exposure and placenta-mediated exposure via sEVs) and the corresponding readouts (ROS formation, mitochondrial activation, and gene expression), was created to improve clarity and accessibility for the reader (Supplemental Fig. S1).

Placental Tissues from Healthy Pregnant Women

Placental tissues were obtained at the Prenatal Diagnosis and Obstetrics Division of the Department of Molecular and Developmental Medicine (University Hospital of Siena, Siena, Italy). Samples at term of gestation ($n = 8$) were collected from elective cesarean sections scheduled for the fetus's cephalic presentation or a previous cesarean. Clinically diagnosed pregnancy disorders, infectious diseases, gestational diabetes, and genetic deficiencies of the fetus were exclusion criteria. Informed consent was obtained from the donors for the collection of placenta samples for research purposes, and approval was obtained from the Ethics Committee of the Azienda Ospedaliera Senese in collaboration with the University of Siena. Within 1 h of collection, the placenta samples were dissected under a microscope to obtain the chorionic villi.

Human Chorionic Villi Culture

After several washes with sterile phosphate-buffered saline (PBS, Cat. No. ECB4004L; EuroClone, Milan, Italy), chorionic villous explants (HPEs) from placental tissues were established as described by Caniggia et al. (33) with minor modifications. Explants ($n = 8$ different placenta) were incubated overnight at 37°C in an atmosphere of 8% O_2, 5% CO_2 in Dulbecco's modified Eagle's medium/Nutrient Mixture F-12 (DMEM F12, w/o phenol red and serum, SH30272.02; Cytiva, Global Life Sciences Solutions) plus L-glutamine (Cat. No. ECB3000D; EuroClone) and 100 U/mL of penicillin-streptomycin (Cat. No. A8943; AppliChem GmbH). The morphology of the explants was constantly monitored under an optical microscope. The medium was then replaced with a fresh one, and placental explants were treated or not (controls) with BPA (Cat. No. 239658; Sigma-Aldrich, St. Louis, MO) 1 nM (powder BPA was dissolved in

EtOH to create a stock solution of 10 mM and diluted at all the finals concentration in proper culture medium) and cultured for 48 h. At the end of the experiments, explant cultures were used to measure viability, ROS production, and protein expression, and their respective supernatants were collected and processed for subsequent analysis.

sEVs Isolation and Characterization

sEVs isolation from placental explants and human brain microvascular endothelial cell line (HBMEC) (Cat. No. P10361; Innoprot, Derio, Spain), which were treated as described in *Cell Culture and Treatments*, was performed as described by Ermini et al. (34). In brief, placenta explant supernatants were centrifuged at 2,500 *g*, at 4°C for 30 min to remove cellular debris and then further spun for 1 h at 15,000 *g* to eliminate the microvesicles. sEVs were then collected by ultracentrifugation (2 h at 100,000 *g*, 4°C). The pellet was resuspended with 1× PBS and centrifuged for 1 h at 100,000 *g* at 4°C. The supernatant was discarded, and the pellet was resuspended with 1 mL of PBS and filtered with a 0.22-μm filter. The most recent Minimal Information for Studies of Extracellular Vesicles (MISEV) recommendations from the International Society for Extracellular Vesicles were followed in the characterization of sEVs (35). Transmission electron microscopy (TEM) to assess sEVs morphology was performed as described by Ermini et al. (36). Quantification of the hydrodynamic diameter distribution and concentration (particles number/mL) of sEVs was performed using the Nanosight NS300 (Malvern Instruments, UK) equipped with a violet laser (405 nm) and running software version NTA3.4. The instrument was primed using PBS, pH 7.4, and the temperature was maintained at 25°C and calibrated using 100- and 200-nm polystyrene beads (Malvern Instruments, UK). sEVs were diluted in 0.1 micron-filtered PBS, and samples were injected into flow cell at a flow rate of 0.05 mL/s through an automated syringe pump. Five measurements (30 s each) were obtained for each sample, and the average was plotted as a representation of size distribution and concentration (particles/mL). For Western blot analyses of canonical [ALG-2 interacting protein X (ALIX), TSG101, CD81, and IRE1α] and placental [Syncytin-1 and placental alkaline phosphatase (PLAP)] sEVs markers, the pellet was resuspended with 40 µL of deionized water (H_2O dd); the used methods are described in *Western Blotting*. In some experiments, isolated placental sEVs were subject to a mechanical disruption performed to disperse their contents. In this case, to rupture the membranes and release their contents, the solution containing the sEVs was sonicated for 10 s, then incubated on ice for 15 min, and the steps repeated three times, before administering the solution with the ruptured sEVs to the cells.

Cell Culture and Treatments

The human glioblastoma astrocytoma (U-373 MG) cell line (Cat. No. 89081403; Sigma-Aldrich) and HBMEC were cultured according to the standard conditions at 37°C in a humidified 5% CO_2 incubator. U-373 MG cells were maintained in DMEM (Cat. No. ECM0728L; EuroClone) supplemented with 10% FBS (Cat. No. ECS5000L; EuroClone), 1% L-glutamine (Cat. No. ECB3000D; EuroClone), and 1% penicillin/streptomycin antibiotics, whereas HBMEC cells were cultured in endothelial cell medium (ECM, Cat. No. P60104; Innoprot) supplemented with 5% FBS (Cat. No. P60104; Innoprot), 1% endothelial cell growth supplement (Cat. No. P60104; Innoprot), and 1% penicillin/streptomycin solution (Cat. No. P60104; Innoprot). Growth medium was refreshed every 2 days, and the cells were subcultured once 80%–90% confluence was reached. All solutions for cell culture were heated to 37°C before use. HBMEC cells (1×10^6 total cells) were seeded in fibronectin (Cat. No. P8248; Innoprot)-coated T-25 cm^2 flasks for sEVs isolation. Cells were either left untreated (control) or treated with 1 nM BPA for 48 h in ECM medium supplemented with 5% sEV-depleted FBS to assess whether the observed effects were specifically placenta-mediated.

U-373 MG cells were cultured, for ROS and *N*-acetyl-L-cysteine (NAC) assay, in 24-well plates (1×10^5 cells/mL), for MitoTracker assay and sEVs incorporation test in glass coverslip in six-well plates (1×10^5 cells/mL), and for Western blot and quantitative real-time PCR in six-well plates (2.5×10^5 cells/mL). Cells were treated or not (controls) initially with BPA at various concentrations (from 0.1 pM to 1 mM) to assess the direct effect of this endocrine disruptor; then, to perform the placenta-mediated experiments, the concentration of BPA 10 nM was chosen and cells were cultured in the same conditions plus sEVs isolated from supernatants of placental explants from $n = 8$ different placentas, and sEVs isolated from HBMEC from $n = 3$ independent experiments. The treatment on U-373 MG was done for 24 h using 3×10^8 vesicles/mL, 60 µL/mL of medium. U-373 MG cells were also treated with 10 µM of H_2O_2 (freshly prepared, Cat. No. 31642; Sigma-Aldrich) as a positive control. Cell viability was determined by trypan blue exclusion assay.

In brief, cells were harvested by trypsinization, resuspended in culture medium, and mixed 1:1 with 0.4% trypan blue solution (Cat. No. T8154; Sigma-Aldrich). Live (unstained) and dead (blue-stained) cells were counted using a Neubauer chamber under light microscopy by two independent operators, and viability was calculated as: (live cells/total cells) × 100.

Measurement of Intracellular ROS

The fluorescence probe 2,7-dichlorodihydrofluorescein diacetate (H_2DCF-DA, Cat. No. D6883; Sigma-Aldrich) was used to detect intracellular ROS at the end of the treatments. In brief, after removing the medium, cells and HPEs were incubated with H_2DCF-DA solution (10 µM in PBS) at 37°C for 15 min and 30 min, respectively.

After incubation, they were washed twice with PBS to remove excess H_2DCF-DA, and the HPEs were also manually homogenized with fresh PBS; fluorescence was measured at excitation and emission wavelengths of 480 and 520 nm, respectively (Synergy HTX Multi-Mode Reader; BioTek, Winooski, VT). The obtained fluorescence values were finally normalized to the number of live cells or total amount of proteins. Average values in control were taken as 100%.

In some experiments, the cell cultures were first treated with NAC (Cat. No. A9165; Sigma-Aldrich), a precursor of glutathione with potent antioxidant action, at 125 µM for 1 h, then added with increasing concentration of BPA (0.1 pM to 1 µM).

Immunofluorescence Analysis

The cell permeable probe MitoTracker Red CMXRos (Cat. No. M7512; Thermo Fisher Scientific, Waltham, MA) was used to detect a loss of membrane potential in mitochondria at the end of treatments. After the medium was removed, the cells were incubated with MitoTracker Red solution (50 µM in DMEM, phenol red-free ECB7504L; Euroclone) at 37°C for 40 min. They were then washed to remove excess MitoTracker Red solution, fixed with 4% paraformaldehyde (Cat. No. 28908; Thermo Fisher Scientific) at 4°C for 10 min and then permeabilized in 0.2% Triton X-100 (Cat. No. T8532; Sigma-Aldrich) in PBS at room temperature for 5 min. The slides were blocked in 5% of bovine serum albumin (Cat. No. A8806; Sigma-Aldrich) at room temperature for 30 min and incubated at 4°C overnight with rabbit anti-TOM20 (diluted 1:250 in PBS, Cat. No. 42406; Cell Signaling Technology, Danvers, MA). After the coverslips were rinsed three times with PBS and incubated 1 h at room temperature with Alexa Fluor 488 goat anti-rabbit IgG secondary antibody diluted 1:500 (Cat. No. A11008; Invitrogen, Basel, Switzerland) in PBS. The slides were then rinsed and mounted with Fluoromount Aqueous Mounting (Cat. No. F4680; Sigma-Aldrich) to avoid fading of fluorescence. Images were acquired on Zeiss LSM700 (Zeiss, Oberkochen, Germany) confocal microscope (magnification = ×63). The different images were analyzed by ImageJ software (Bethesda, MD).

For mitochondrial fluorescence analysis, confocal images were analyzed using ImageJ software (NIH, version 1.53). Specifically: *1*) individual cells were outlined as regions of interest (ROIs); *2*) mean gray values for MitoTracker Red and TOM20 channels were measured for each ROI; *3*) background fluorescence was subtracted; *4*) the ratio of MitoTracker Red/TOM20 was calculated for each cell; and *5*) colocalization was assessed using the JACoP plugin, calculating Pearson's correlation coefficient. At least 30 cells per condition from three independent experiments were analyzed. To investigate the possible uptake of sEVs from the placenta by astrocytes, sEVs were labeled with the PKH67 Fluorescent Cell Linker Kit (Cat. No. PKH67GL-1KT; Sigma-Aldrich) as described by Ermini et al. (34). The labeled sEVs were pelleted at 120,000 *g* for 1 h and resuspended in PBS. The spin and wash cycles were repeated three times. Cells with a confluence of 60%–70% were treated with 60 µL/mL of labeled sEVs (5 × 108 vesicles) for 3, 6, and 18 h. Cells were then fixed with 4% paraformaldehyde, and images were captured using an LSM700 confocal microscope (Zeiss).

Isolation of RNA and Quantitative Real-Time PCR

Total RNA from the U-373 MG cell culture (treated as previously described) was isolated using the Zymo-Spin I Fast-Spin column (Cat. No. C1003; Zymo-Research, Irvine, CA) according to the manufacturer's instructions. Total RNA was quantified using the Nanodrop 1000 Spectrophotometer (Thermo Fisher Scientific). RNA was reversed-transcribed into cDNA using the High-Capacity cDNA Reverse Transcription Kit (Cat. No. 4368814; Applied Biosystems Group, Foster City, CA). Quantitative real-time PCR (qRT-PCR) reactions were run in the StepOne Real-Time PCR System instrument (Applied Biosystems Group). cDNA was amplified using the iQTM SYBR Green Supermix (Bio-Rad, Hercules, CA). Predeveloped primers for SOD1, GCLC, GSTA, CCL2, and IL-1β (Bio-Rad) were used for relative quantification of mRNA; GAPDH and 18S (Bio-Rad) were used as housekeeping genes (Supplemental Table S1). The expression level of the selected genes was calculated by the $2^{-\Delta\Delta Ct}$ method, using the geometric mean of the two reference genes (GAPDH and 18S) for normalization (37).

Western Blotting

Western blot was performed on HPEs, U-373 MG, and sEVs. Cells and HPEs were homogenized with RIPA buffer (Cat. No. 20-188; Sigma-Aldrich) and phosphatase inhibitors (Cat. No. P5726; Sigma-Aldrich) (1:100), and 30 µg of total proteins were loaded. After the last ultracentrifugation, sEVs pellet was resuspended with 40 µL of H_2O dd and stored at −80°C. Western blots were performed on 8%, 10%, and 15% gels systems. Electrophoresis was performed at a constant 135 V for 1 h and 10 min. Proteins were transferred onto a nitrocellulose membrane (Bio-Rad) for 2 h at a constant 400 V. After transfer, membranes were incubated in 5% nonfat milk in PBS-0.1% Tween-20 (Cat. No. P9416; Sigma-Aldrich) for 1 h at room temperature. Subsequently, membranes were incubated in primary antibodies overnight at 4°C. The following antibodies were used for HPEs: SYNCYTIN1 (ERVW-1, Cat. No. SAB2108833, diluted 1:500; Sigma-Aldrich); for U-373 MG: SLC1A5 (Cat. No. ab237704, diluted 1:1,000; Abcam, Cambridge, UK) and GAPDH (Cat. No. G8795, diluted 1:1,000; Sigma-Aldrich); and for sEVs: ALIX (Cat. No. ZRB1947, diluted 1:500; Sigma-Aldrich), SYNCYTIN1 (ERVW-1, Cat. No. SAB2108833, diluted 1:500; Sigma-Aldrich), PLAP (Cat. No. ab16695, diluted 1:500; Abcam), TSG101 (Cat. No. T5701, diluted 1:500; Sigma-Aldrich), CD81 (Cat. No. HPA007234, diluted 1:200; Sigma-Aldrich), and IRE1α (Cat. No. 3294, diluted 1:500; Cell Signaling Technology).

Membranes were washed and incubated with the appropriate secondary peroxidase labeled antibody for 1 h at room temperature at a dilution of 1:3,000 (Bio-Rad). The reaction was detected using chemiluminescent reagents (Cat. No. 170-5060, Clarity Western ECL Substrate; Bio-Rad) and digitized with CHEMIDOC Quantity One 1-D Analysis Software. Densitometries were carried out using ImageJ software (NIH Image; https://imagej.nih.gov/ij/).

Statistical Analyses

sEVs were isolated from $n = 8$ different placental donors. Each experiment (ROS measurement, gene expression, Western blot, and immunofluorescence) was then repeated independently three to seven times using sEVs preparation (3 biological replicates), each performed on different days with freshly cultured cells. Cell-based experiments were performed with three independent biological replicates (different cell passages), each performed in technical duplicate. qRT-PCR measurements were performed in technical duplicate for each biological replicate.

All datasets were first analyzed for normality using the Shapiro–Wilk test (for $n < 50$) or Kolmogorov–Smirnov test (for $n \geq 50$). A P value >0.05 in these tests indicated normal distribution. For normally distributed data with equal variances (assessed by Levene's test), parametric tests were used: unpaired t test for two-group comparisons, and one-

way ANOVA followed by Dunnett's or Bonferroni post hoc tests for multiple comparisons. All our data met normality assumptions; therefore, only parametric tests were used. The level of significance was set at $P < 0.05$. Statistical analyses were performed using GraphPad Prism 8 (GraphPad Software, San Diego, CA).

RESULTS

Direct Exposure to BPA Alters ROS Production and Viability in Astrocytes

Since ROS and mitochondria play an important role in astrocyte cell death, the potential damaging effect of BPA on astrocytes was investigated by simultaneously assessing ROS and cell viability. We tested a wide range of BPA concentrations, starting at 0.1 pM up to 1 mM. As shown in Fig. 1*A*, direct BPA exposure at 10 nM began to significantly increase ROS production, with a greater effect at concentrations of 100 nM and 1 μM compared with untreated cells. Although 10 nM BPA had no effect on cell viability (86%), the higher ROS rates at the 100 nM and 1 μM concentrations correlated with lower cell viability (62% and 56%, respectively) (Fig. 1*B*). Thus, we hypothesized that the increase in ROS production found in BPA at 100 nM and 1 μM was due to mitochondria damage and passive release of ROS. To confirm this hypothesis, cells were pretreated with NAC, a known reactive oxygen scavenger, for 1 h. The results showed that the NAC treatment significantly restored cell viability in 1 μM and 100 nM BPA cultures as well as in H_2O_2 treatment and decreased ROS production in 10 nM, 100 nM, 1 μM, and H_2O_2 cultures, emphasizing the importance of ROS in causing damage and cell death in astrocytes (Fig. 1, *C* and *D*).

Direct Exposure to BPA Alters Mitochondrial Activation

We then examined mitochondrial function by analyzing active and total mitochondria with MitoTracker Red and TOM20, respectively. For this test, we used the concentration of 10 nM because, as shown previously, it was nontoxic and increased ROS generation. Using MitoTracker Red, which localizes to the mitochondria and whose signal intensity depends on the mitochondrial membrane potential, we observed a significant increase in fluorescence intensity in the cells treated with BPA, whereas no changes were observed for TOM20 compared with the control (Fig. 2, *A* and *B*). On this basis, the ratio of fluorescence intensity (MitoTracker Red/TOM20) was increased ($P < 0.005$), suggesting that although the total amount of mitochondria did not change, the number of active mitochondria was increased in the BPA-treated cells compared with the control. These data were further confirmed by colocalization analysis of MitoTracker and TOM20 labeling using ImageJ's JACoP tool, which showed a substantial correlation between the two stains in BPA-treated cells (Pearson's correlation, PC = 0.90) and a low degree of colocalization in unexposed cells (PC = 0.7).

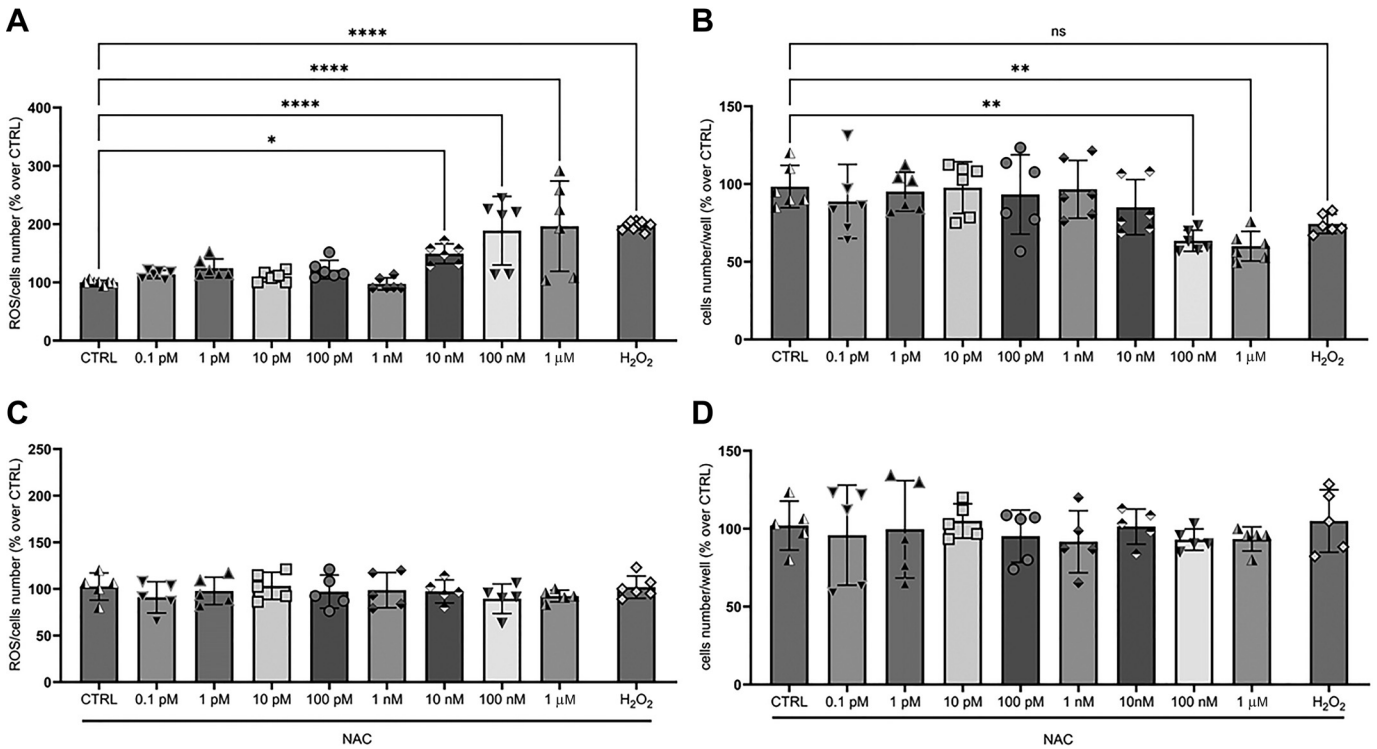

Figure 1. Effects of different concentrations of BPA exposure on oxidative stress by formation of ROS in U-373 MG cells. *A*: ROS formation was evaluated by the oxidation of H_2DCF-DA to DCF on cells subjected to the BPA treatment protocol (1 μM to 0.1 pM) for 24 h. *B*: cellular viability was evaluated by cell count. *C*: ROS formation in astrocytes treated with BPA (1 μM to 0.1 pM) and NAC 125 μM. *D*: cellular viability was evaluated by cell count. Data are reported as means ± SD from six and five independent experiments, each carried out in duplicate. *$P < 0.05$; **$P < 0.01$; ****$P < 0.0001$ vs. untreated cells (CTRL; 1-way ANOVA and Dunnett's multiple comparisons test). BPA, bisphenol A; H_2DCF-DA, 2,7-dichlorodihydrofluorescein diacetate; NAC, *N*-acetyl-L-cysteine; ns, not significant; ROS, reactive oxygen species; U-373 MG, human glioblastoma astrocytoma.

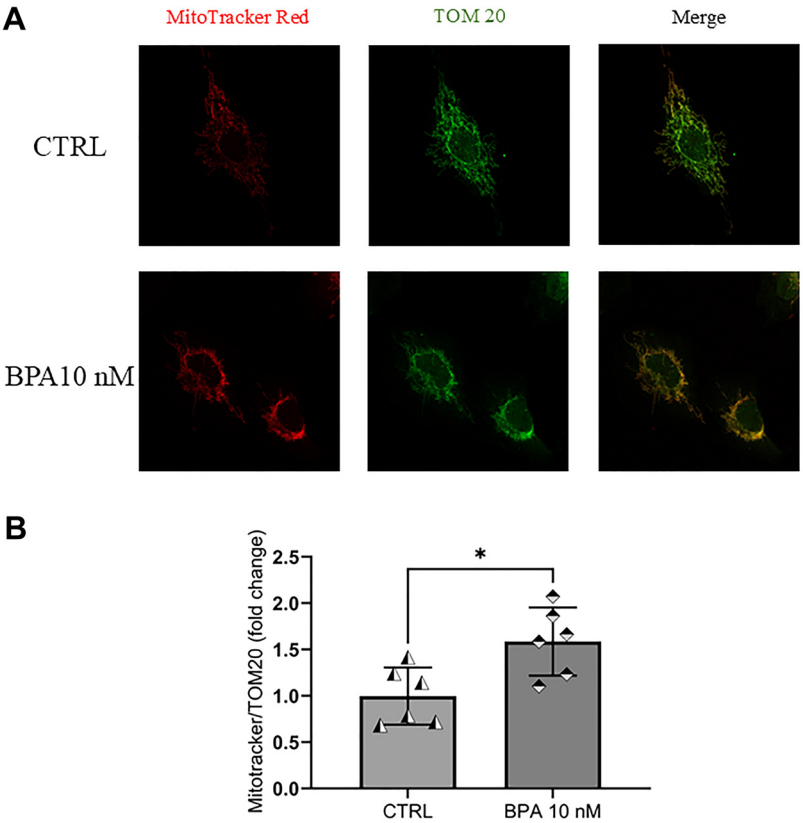

Figure 2. Effects of 10 nM BPA exposure on mitochondrial activation in U-373 MG cells. *A*: representative fluorescence images of mitochondrial activation were evaluated by treatment with MitoTracker Red on cells subjected to the 10 nM BPA treatment for 24 h. Magnification = ×63. Each image was representative of six independent experiments. *B*: fluorescence amount ratio between MitoTracker Red and TOM20 (green) by ImageJ JACoP tool. Data are reported as means ± SD from six independent experiments; $*P < 0.05$ (*t* test). Bar = 8 µm. BPA, bisphenol A; U-373 MG, human glioblastoma astrocytoma.

Direct Exposure to BPA Alters ROS Production and SYNC Levels in Human Placenta Explants

In parallel, we assessed the redox state of the placenta by preparing and culturing HPEs derived from placentas of healthy donors following cesarean delivery. The explants were cultured under physiological conditions (CTRL) and exposed to 1 nM BPA for 48 h. As shown in Fig. 3*A*, exposure to 1 nM BPA significantly increased the production of ROS compared with the untreated explants. Subsequently, we

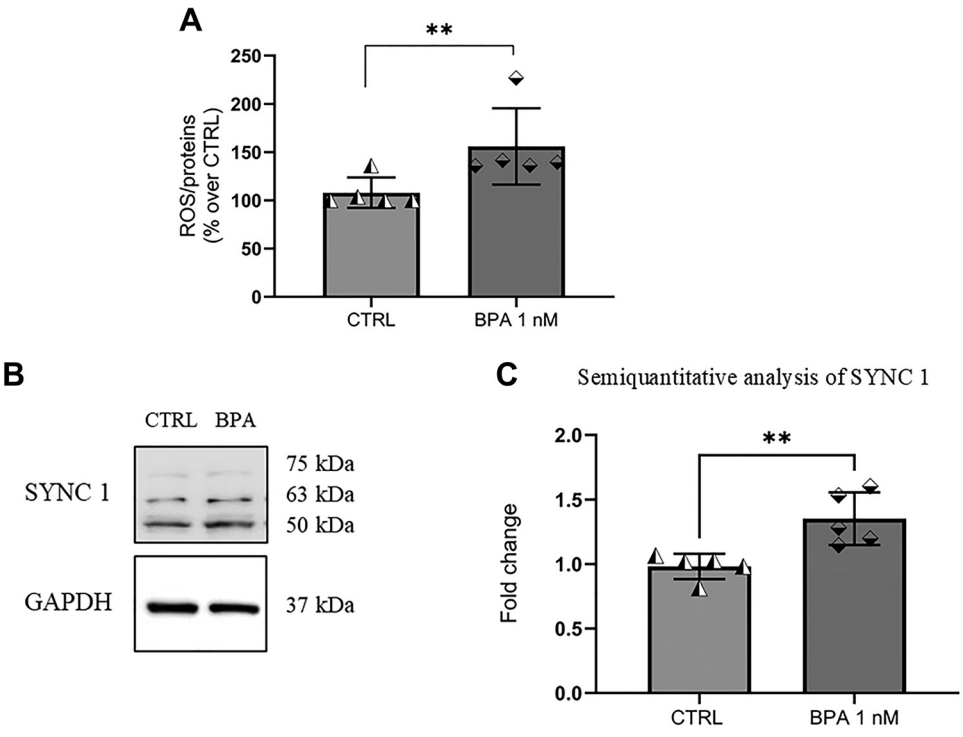

Figure 3. Effects of 1 nM BPA exposure on oxidative stress and SYNC1 levels on human placenta explants. *A*: ROS formation was evaluated by the oxidation of H_2DCF-DA to DCF on human placenta explants (HPEs) after 48 h of ex vivo culture in control and 1 nM BPA exposure conditions. *B*: representative Western blot of SYNC1 and GAPDH in HPEs after 48 h of ex vivo culture in control and 1 nM BPA exposure conditions. *C*: semiquantitative analysis of Western blot. Data are reported as means ± SD from five independent experiments; $**P < 0.01$ (*t* test). BPA, bisphenol A; H_2DCF-DA, 2,7-dichlorodihydrofluorescein diacetate; ROS, reactive oxygen species; SYNC1, Syncytin-1.

analyzed the levels of SYNC following treatment. Notably, fold-change analysis, normalized to GAPDH, revealed that SYNC protein levels were significantly higher in BPA-exposed HPEs than in the controls (Figs. 3, *B* and *C*).

sEVs Isolation and Characterization

Subsequently, we started to evaluate the placental-mediated effect of BPA exposure. For this purpose, we collected HPEs secretome for sEVs isolation by ultracentrifugation. The presence of membrane vesicles in both samples, BPA-sEVs and CTRL-sEVs, was confirmed by transmission electron microscopy (TEM) (Fig. 4*A*). As shown in Fig. 4*B*, nanoparticle tracking analysis performed using the Nanosight NS300 (Malvern Instruments, UK) revealed an average particle concentration of $4 \times 10^{10} \pm 1.0 \times 10^{10}$ particles/mL for CTRL-sEVs and $4.4 \times 10^{10} \pm 0.6 \times 10^{9}$ particles/mL for BPA-sEVs with a mode of 95 ± 20 nm and 110 ± 10 nm, respectively. Both sEVs samples expressed the typical EVs marker proteins, including ALG-2 interacting protein X (ALIX), tumor susceptibility gene 101 (TSG101) and those indicative of a trophoblastic origin such as placental alkaline phosphatase (PLAP) and Syncytin-1 (SYNC) (Fig. 4*C*). As recommended by the International Society for Extracellular Vesicles (MISEV) guidelines, the purity of sEVs isolation was further evaluated by Western blot analysis for IRE1α, used as a marker of intracellular membrane contamination.

Interestingly, fold-change analysis normalized to Ponceau staining revealed that SYNC protein levels were significantly higher in BPA-sEVs than in CTRL-sEVs (Fig. 4*D*).

Placental sEVs Incorporation in U-373 MG

We then examined the uptake of sEVs by U-373 MG. First, we assessed the levels of the SLC1A5 receptor after exposure to BPA 10 nM (Fig. 5*A*); this receptor is important for the transport of neutral amino acids such as glutamine, serine, and alanine and is involved in Syncytin-1 binding; the treatment with BPA 10 nM does not alter the expression of this receptor, as shown by the semiquantitative analysis in Fig. 5*B*. In parallel, in a time-course study, a total of 60 µL/mL of PKH67-labeled CTRL-sEVs and BPA-sEVs (5 × 108 vesicles) were added to astrocyte cultures. Confocal images revealed the presence of fluorescent particles of CRTL-sEVs and BPA-sEVs within the cells; however, the incorporation into astrocytes of BPA-sEVs was greater than that of CTRL-sEVs at all time points tested, with a significant difference at 3 h after treatment (Fig. 5*D*).

Placenta-Mediated Exposure to BPA Restores REDOX Equilibrium Increasing Antioxidant Enzymes Expression in U-373 MG

To test the effect of the placental secretome on astrocytes exposed to BPA, we analyzed ROS formation following combined treatments with placental sEVs and BPA 10 nM. After 24 h, the redox balance of astrocytes was restored compared with the BPA 10 nM group, returning to physiological levels (CTRL baseline, corresponding to the untreated control—CTRL—values reported in Figs. 1 and 6*A*), with no significant changes in cell viability (Fig. 6*B*), regardless of whether the sEVs originated from BPA-exposed or control placental cultures.

This protective effect appeared to be placenta-specific, since cotreatment with BPA 10 nM and sEVs derived from HBMEC cultures failed to mitigate ROS accumulation (Supplemental Fig. S2).

On the contrary, this double exposure, BPA plus BPA-sEVs, led to an upregulation of mRNA expression levels of antioxidant enzymes, including SOD1, GSTA, and GCLC, compared with treatment with BPA alone, suggesting that placental sEVs may activate compensatory antioxidant responses in astrocytes. Interestingly, mechanical disruption of placental sEVs before cell treatment did not result in upregulation of mRNA expression of antioxidant enzymes (Fig. 6*C*).

Placenta-Mediated Exposure to BPA Restores Mitochondrial Activation

Furthermore, the combined treatments with placental sEVs and BPA 10 nM could also restore the energetic status of mitochondria that returns to physiological levels after BPA exposure (CTRL baseline, corresponding to the untreated control–CTRL–values reported in Figs. 2 and 7*A*). Indeed, double labeling with MitoTracker Red and TOM20 showed a significant decrease in MitoTracker staining in cells exposed to BPA plus BPA-sEVs compared with treatment with 10 nM BPA, with the Pearson's coefficient decreasing from 0.9 for 10 nM BPA to 0.7 for sEVs-treated cells. This was accompanied by a significant decrease in the MitoTracker Red/TOM20 ratio (Fig. 7*B*).

Placenta-Mediated Exposure to BPA Modulates Cellular Responses to Stress and Inflammation

In addition, we investigated the functional role of regulation of the redox state of astrocytes by placental sEVs by analyzing the mRNA expression of cytokines and chemokines important for homeostasis in the CNS. Interestingly, exposure to 10 nM BPA in the presence of sEVs isolated from placental explants exposed to BPA significantly reduced CCL2 and IL-1β expression compared with treatment with BPA alone, which return to physiological levels (Fig. 8), suggesting that the uptake observed for BPA-sEVs may be responsible for this effect.

DISCUSSION

This study demonstrates that exposure to the endocrine disruptor BPA, even at low doses (1 and 10 nM), which are actually present in human blood (38), causes significant effects on cellular metabolism and redox homeostasis in human placenta and astrocytes, respectively.

BPA-Induced Oxidative Stress in Astrocytoma Cells

We first evaluated the direct effect of BPA exposure on the redox status of astrocytes. We found that BPA exposure results in a nonphysiological increase in ROS not only at the highest concentrations, which are not compatible with cell life in vitro, but also at the highest dose that was not cytotoxic, which had not been studied previously. In fact, treating the cells with NAC, a known precursor of reduced glutathione, a molecule critical for maintaining oxidative balance, significantly reduced BPA-induced ROS production and restored cell viability. This suggests that the ROS

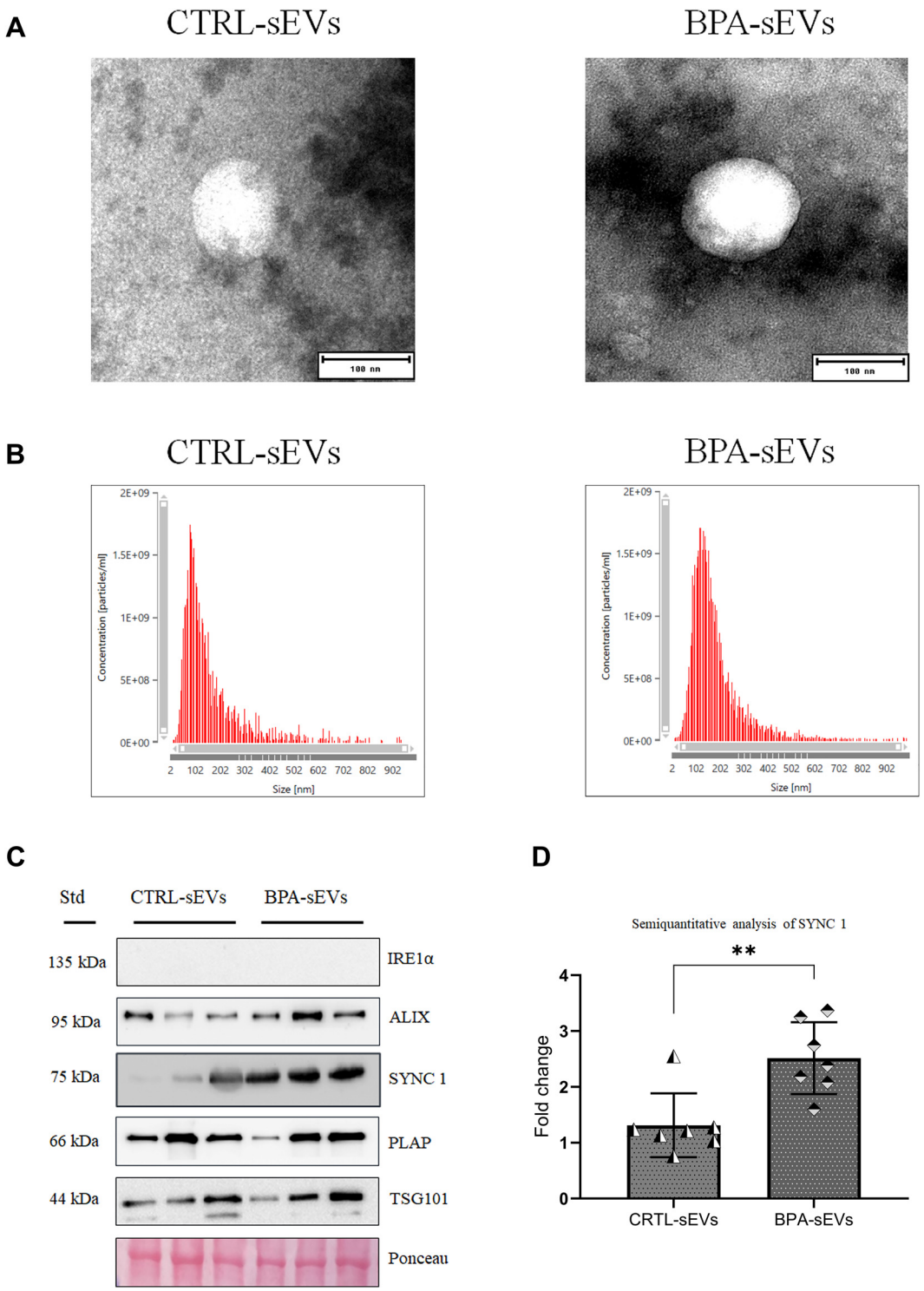

Figure 4. Placental sEVs visualization and characterization. *A*: transmission electron microscopy analysis of sEVs isolated from HPE medium after 48 h of ex vivo culture (CTRL and BPA 1 nM). Bar = 100 nm. *B*: Nanosight NS300 analysis of sEVs isolated from the HPE medium after 48 h of ex vivo culture (CTRL and BPA 1 nM). *C*: representative Western blot of IRE1α, ALIX, SYNC1, PLAP, and TSG101 in sEVs isolated from HPEs after 48 h of ex vivo culture in control and 1 nM BPA exposure conditions. *D*: semiquantitative analysis of SYNC1 protein levels normalized to Ponceau staining. Data are reported as means ± SD from seven independent experiments; $^{**}P < 0.01$ (*t* test). ALIX, ALG-2 interacting protein; BPA, bisphenol A; HPEs, human placenta explants; PLAP, placental alkaline phosphatase; sEVs, small extracellular vesicles; SYNC1, Syncytin-1; TSG101, tumor susceptibility gene 101.

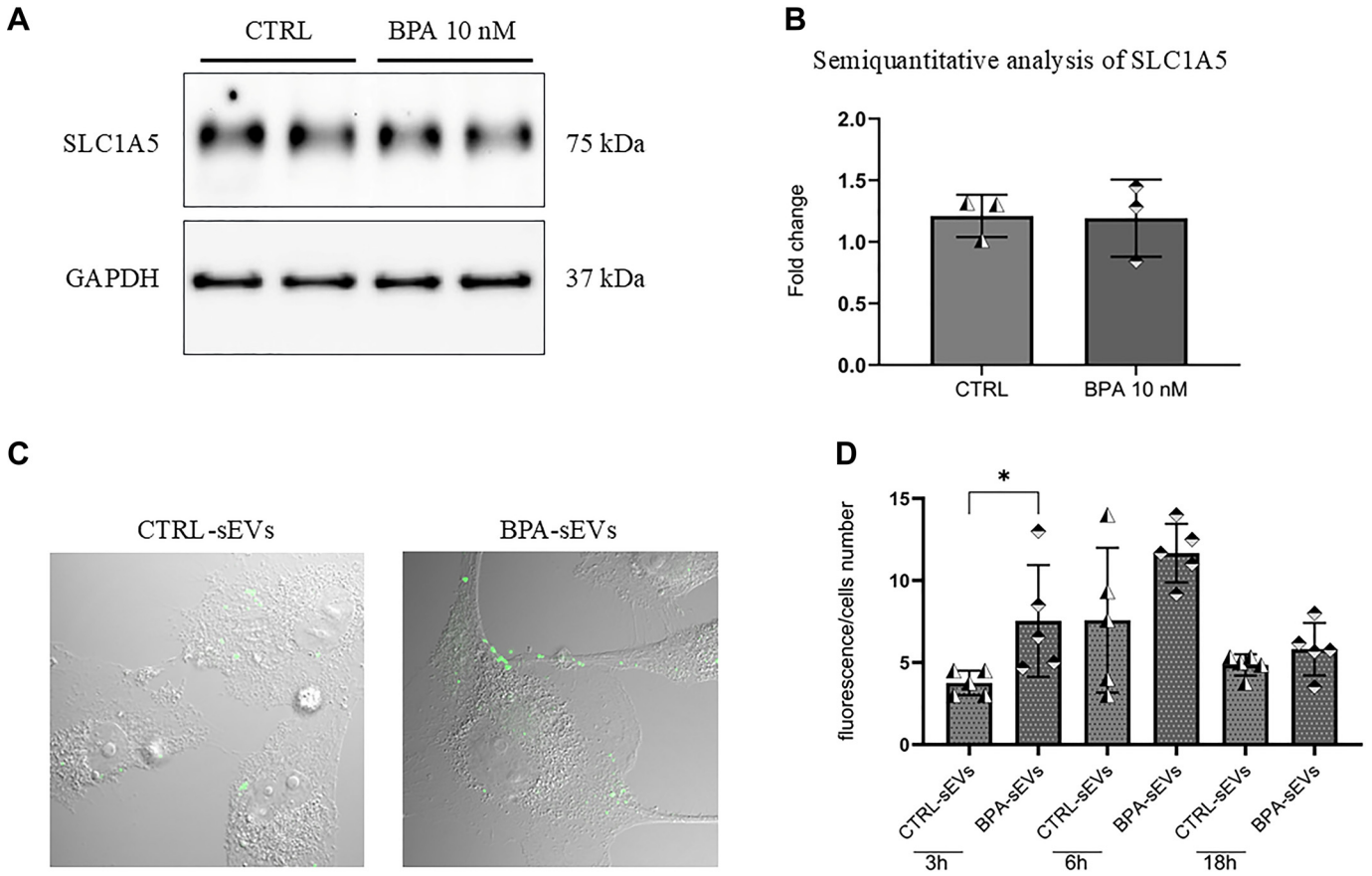

Figure 5. Placental sEVs incorporation by U-373 MG cells. *A*: representative Western blot of SLC1A5 and GAPDH in U-373 MG after 24 h of culture in control and 10 nM BPA exposure conditions. *B*: semiquantitative analysis of Western blot. *C*: representative images of CTRL-sEVs and BPA-sEVs incorporation labeled placental sEVs with PKH67 Green linker. Magnification = ×63. Bar = 8 μm. *D*: relative semiquantification (mean gray value of fluorescence) calculated with ImageJ. Data are reported as means ± SD from three and five independent experiments, each carried out in duplicate. *$P < 0.05$ vs. CTRL-sEVs (*t* test). BPA, bisphenol A; sEVs, small extracellular vesicles; U-373 MG, human glioblastoma astrocytoma.

increase is redox-dependent. The protective effect of NAC indicates that the observed redox imbalance is potentially reversible, highlighting oxidative stress as a key mechanism through which BPA exerts cellular toxicity; in fact, reducing the amount of ROS increase cells viability. Furthermore, exposure to 10 nM BPA resulted in increased ROS production and a higher degree of mitochondrial activation. This could be linked to decreased functionality of the electron transport chain and reduced ATP production efficiency (39).

Placental Responses to BPA Exposure

In the case of placental explants, exposure to 1 nM BPA for 48 h resulted in an increase in ROS. However, the viability of the explants remained unchanged, suggesting that BPA may alter the cellular defense mechanisms against oxidative stress, even at levels considered safe. Concurrently, there was an increase in the expression of Syncytin-1, encoded by ERVW-1, a crucial protein involved in the cell-cell fusion of cytotrophoblasts (40, 41). On the contrary, this exposure did not alter the sEVs production, which remained consistent in both concentration and size (42). These vesicles contain a variety of proteins, lipids, small amounts of DNA, and different RNA species (e.g., mRNA and microRNA), including mRNAs encoding antioxidant enzymes, such as superoxide dismutase (SOD), catalase, and glutathione peroxidase (43). These enzymes are essential for neutralizing ROS and mitigating oxidative stress. By encapsulating these mRNAs within sEVs, the placenta may activate protective mechanisms and deliver genetic instructions to target cells, enhancing their antioxidant defenses in response to oxidative challenges like those induced by BPA exposure.

sEVs-Mediated Protection Mechanisms

It is also important to note that the presence of specific surface proteins or putative ligands that likely bind to receptors on target cells, although these ligands and target cells remain largely unidentified, is critical for the proper recognition and uptake of these vesicles. In particular, we observed an increase in Syncytin-1 levels not only in HPEs but also on sEVs membranes. Syncytin-1 plays a role in the uptake of vesicles by facilitating their fusion with recipient cell membranes, which are equipped with its receptor, SLC1A5, ensuring that the vesicular cargo is effectively delivered to the target cells (44).

This shows why sEVs from BPA-exposed explants (BPA-sEVs) had a higher incorporation profile than those produced from physiological explants (CTRL-sEVs), even though SLC1A5 receptor levels on astrocytes did not change.

The release of sEVs containing antioxidant factors enables intercellular communication and may contribute to the

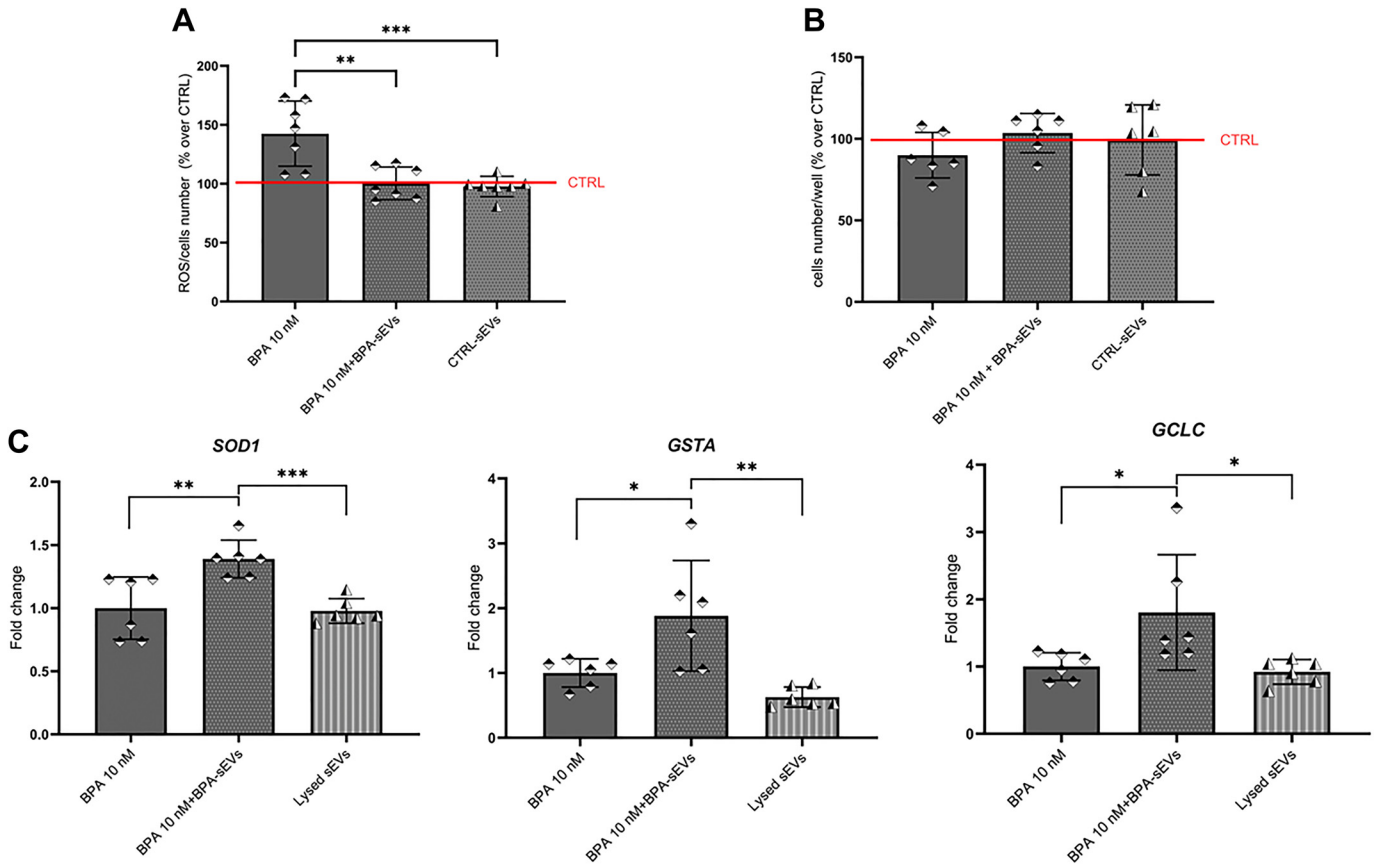

Figure 6. Effects of placenta-mediated BPA exposure on oxidative status in U-373 MG cells. *A*: ROS formation was evaluated by the oxidation of H_2DCF-DA to DCF on cells treated with BPA 10 nM, BPA 10 nM + BPA-sEVs, and CTRL-sEVs as described in MATERIALS AND METHODS. *B*: cell viability: cells were treated as described in MATERIALS AND METHODS. *C*: SOD1, GSTA, and GCLC mRNA expression after 24 h of 10 nM BPA + BPA-sEVs treatment and lysed sEVs. Data are reported as means ± SD from six and seven independent experiments, each carried out in duplicate; $^{*}P < 0.05$; $^{**}P < 0.01$; $^{***}P < 0.001$ vs. 10 nM BPA-treated cells (BPA, 10 nM; 1-way ANOVA and Dunnett's multiple comparisons test). BPA, bisphenol A; H2DCF-DA, 2,7-dichlorodihydrofluorescein diacetate; ROS, reactive oxygen species; sEVs, small extracellular vesicles; U-373 MG, human glioblastoma astrocytoma.

cellular response to stressors by enhancing the antioxidant capacity of cells through the transfer of protective factors. Interestingly, our findings suggest that sEVs counteract the harmful effects of BPA, and the increased fusion efficiency facilitates the transfer of protective molecules to astrocytes, helping restore redox balance and prevent mitochondrial damage.

ROS as Signaling Molecules and Implications for Neuroinflammation

Mitochondria are considered the major source of intracellular ROS, which are mainly produced as a consequence of electron leak from the electron transport chain during the oxidative phosphorylation. ROS have two opposing effects on cells. Excessive ROS can react with vital components of the cell, including membranes, proteins, and nucleic acids, including the mitochondrial DNA leading to oxidative damage and ultimately cell death (45). On the contrary, at physiological concentrations, ROS functions as second messengers in a variety of signaling pathways and cellular and mitochondrial functions. During recent years, considerable experimental evidence has emerged supporting the role of ROS as signal molecules (43–45). At moderate concentrations, ROS actively participate in a variety of complex biological processes involved in normal cell growth, such as signal transduction, control of gene expression, cell senescence, and apoptosis. The downstream cellular targets of ROS have long been studied, and despite considerable progress in recent years, they have not yet been fully defined. ROS can directly regulate the activity of transcription factors, which depends, at least in part, on the redox state of cells (46), including pathways that regulate the expression of inflammatory cytokines and chemokines such as CCL2 and IL-1β. These mediators play critical roles in both acute and chronic inflammatory responses, and their production and activity are closely linked to inflammatory and immunological responses, particularly in the CNS. In astrocytes, CCL2 and IL-1β are key factors in neuroinflammation. CCL2 is involved in the recruitment of monocytes and other immune cells to sites of injury or infection, and it can contribute to the progression of neuroinflammatory diseases by promoting the infiltration of peripheral immune cells into the brain. IL-1β, a potent proinflammatory cytokine, is produced by astrocytes in response to various stressors, including oxidative stress, and plays a significant role in the activation of microglia and other glial cells.

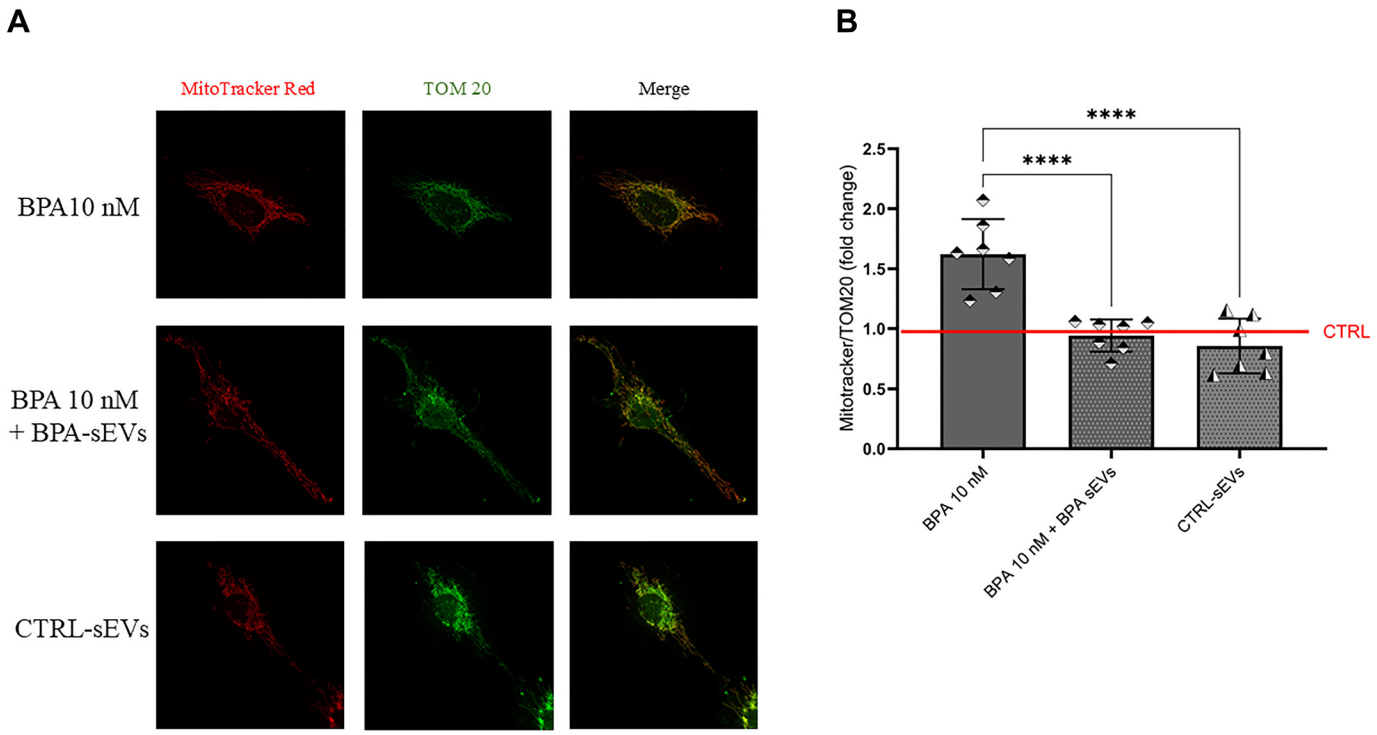

Figure 7. Effects of placenta-mediated exposure of BPA on mitochondrial activity and gene expression in U-373 MG cells. *A*: representative fluorescence images of changes in the mitochondrial membrane potential, as assessed by MitoTracker Red (red) and anti-TOM20 (green) staining in cells subjected to BPA 10 nM + placenta sEVs treatment protocol. Magnification = ×63. Bar = 8 µm. Each photograph was representative of at least three independent observations. *B*: fluorescence amount ratio between MitoTracker Red and TOM20 (green) by ImageJ JACoP tool. Data are reported as means ± SD from seven independent experiments, each carried out in duplicate. ****$P < 0.0001$ vs. 10 nM BPA-treated cells (BPA, 10 nM; 1-way ANOVA and Dunnett's multiple comparisons test). BPA, bisphenol A; sEVs, small extracellular vesicles; U-373 MG, human glioblastoma astrocytoma.

Implications for Fetal Neuroprotection and Study Limitations

Given the central role of ROS in cellular function, it is crucial to understand how exposure to BPA may disrupt these processes, particularly during critical stages of prenatal development, and in particular for the proper formation of the CNS. This system is among the organs most susceptible to this type of insult. This happens because ROS can decrease synaptic plasticity, altering the formation of proper neuronal signals (21, 47). Indeed, oxidative stress has been linked in the etiopathogenesis of many diseases, such as autism spectrum conditions and neurodevelopmental delays (22). The increase in research in recent years on some endocrine disruptors, such as BPA, has revealed links between BPA-induced oxidative stress and human disease (23). The

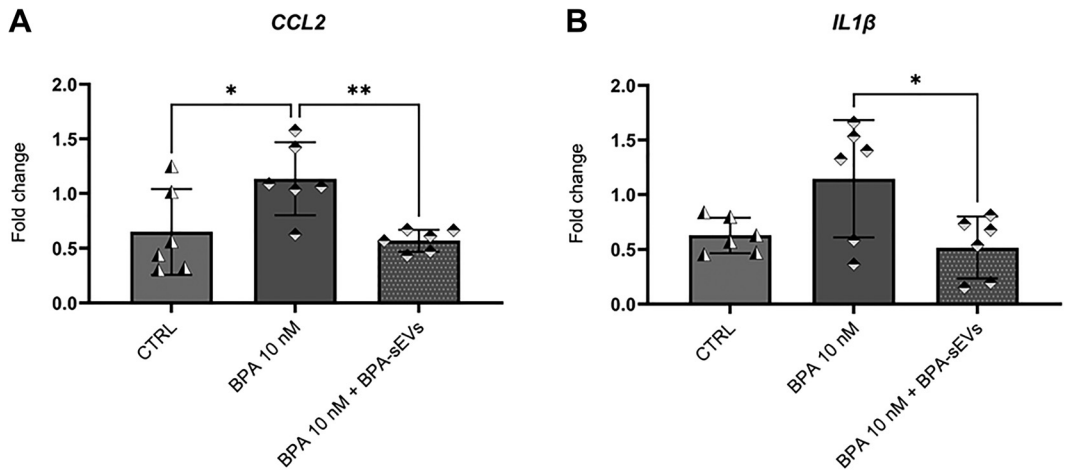

Figure 8. Effects of 10 nM BPA + BPA-sEVs exposure on CCL2 and IL-1β gene expression in U-373 MG cells. *A* and *B*: CCL2 and IL-1β mRNA expression after 24 h of 10 nM BPA + BPA-sEVs treatment. Data are reported as means ± SEM from six independent experiments, each carried out in duplicate; *$P < 0.05$; **$P < 0.01$ vs. 10 nM BPA-treated cells (BPA, 10 nM; 1-way ANOVA and Dunnett's multiple comparisons test). BPA, bisphenol A; sEVs, small extracellular vesicles; U-373 MG, human glioblastoma astrocytoma.

novelty of this study lies in demonstrating that placental sEVs can modulate astrocyte responses to BPA-induced oxidative stress at environmentally relevant concentrations. Despite the known toxic effects of BPA on cellular redox balance, our findings suggest that the placenta might play an essential role in buffering oxidative stress and protecting the developing brain, particularly through the secretion of sEVs containing antioxidant factors. These vesicles may help in restoring redox homeostasis in astrocytes, thus providing a protective mechanism for the fetus.

It is important to note, however, that although this study focuses on fetal astrocytes, we cannot exclude the possibility that the protective effects observed could extend to the mother as well.

In fact, once in the circulation, these sEVs can potentially reach the maternal CNS, cross the blood-brain barrier and exert a significant influence on the overall neuroinflammatory environment (48). This could be particularly relevant in conditions where maternal neuroinflammation or neurodegeneration is present. Given the potential role of sEVs in cellular communication, it is plausible that the placental release of these vesicles in response to BPA exposure could help buffer maternal oxidative stress, ultimately aiding in the maintenance of normal brain function during pregnancy.

Future Directions

Future studies must continue to explore the long-term consequences of prenatal BPA exposure on fetal health, with a focus on the potential for adverse outcomes related to oxidative stress and inflammation.

In addition, future research should explore whether this protective mechanism extends beyond the fetus to influence maternal neurobiology, offering a more comprehensive understanding of how placental-derived factors may support the health of both the mother and the developing child.

Understanding the dynamic interaction between the placenta, fetal cells, and maternal systems is crucial for developing effective strategies to mitigate the impact of environmental chemicals on pregnancy outcomes and long-term health.

DATA AVAILABILITY

The raw data supporting the conclusions of this article will be made available by the authors, without undue reservation.

SUPPLEMENTAL MATERIAL

Supplemental Figs. S1 and S2 and Supplemental Table S1: https://doi.org/10.6084/m9.figshare.30565553.

GRANTS

This work was supported by “Next-Generation EU, Missione 4 Componente 1” CUP: B53D23021400006; FCUR2022 (CUP B65F21002780001); and PSR 2022 from the University of Siena.

DISCLOSURES

No conflicts of interest, financial or otherwise, are declared by the authors.

AUTHOR CONTRIBUTIONS

L.E. and F.I. conceived and designed research; S.N., A.P., S.P., R.R., and L.C. performed experiments; S.N., C.B., L.E., and F.I. analyzed data; S.N., L.E., and F.I. interpreted results of experiments; S.N., S.P., S.C., L.E., and F.I. prepared figures; S.N., L.E., and F.I. drafted manuscript; F.M.S., L.E., and F.I. edited and revised manuscript; F.I. approved final version of manuscript.

REFERENCES

1. **Khalili Sadrabad E**, **Hashemi SA**, **Nadjarzadeh A**, **Askari E**, **Akrami Mohajeri F**, **Ramroudi F.** Bisphenol A release from food and beverage containers – a review. *Food Sci Nutr* 11: 3718–3728, 2023. doi:10.1002/fsn3.3398.
2. **Nelson W**, **Liu D-Y**, **Yang Y**, **Zhong Z-H**, **Wang Y-X**, **Ding Y-B.** In utero exposure to persistent and nonpersistent endocrine-disrupting chemicals and anogenital distance. A systematic review of epidemiological studies†. *Biol Reprod* 102: 276–291, 2020. doi:10.1093/biolre/ioz200.
3. **Sifakis S**, **Androutsopoulos VP**, **Tsatsakis AM**, **Spandidos DA.** Human exposure to endocrine disrupting chemicals: effects on the male and female reproductive systems. *Environ Toxicol Pharmacol* 51: 56–70, 2017. doi:10.1016/j.etap.2017.02.024.
4. **Darbre PD.** Endocrine disruptors and obesity. *Curr Obes Rep* 6: 18–27, 2017. doi:10.1007/s13679-017-0240-4.
5. **Ribeiro E**, **Ladeira C**, **Viegas S.** Occupational exposure to bisphenol A (BPA): a reality that still needs to be unveiled. *Toxics* 5: 22, 2017. doi:10.3390/toxics5030022.
6. **Valentino R**, **D'Esposito V**, **Ariemma F**, **Cimmino I**, **Beguinot F**, **Formisano P.** Bisphenol A environmental exposure and the detrimental effects on human metabolic health: is it necessary to revise the risk assessment in vulnerable population? *J Endocrinol Invest* 39: 259–263, 2016. doi:10.1007/s40618-015-0336-1.
7. **Michałowicz J.** Bisphenol A – sources, toxicity and biotransformation. *Environ Toxicol Pharmacol* 37: 738–758, 2014. doi:10.1016/j.etap.2014.02.003.
8. **Gao X**, **Wang H-S.** Impact of bisphenol A on the cardiovascular system — epidemiological and experimental evidence and molecular mechanisms. *Int J Environ Res Public Health* 11: 8399–8413, 2014. doi:10.3390/ijerph110808399.
9. **Delfosse V**, **Grimaldi M**, **Le Maire A**, **Bourguet W**, **Balaguer P.** Nuclear receptor profiling of bisphenol-A and its halogenated analogues. *Vitam Horm* 94: 229–251, 2014. doi:10.1016/B978-0-12-800095-3.00009-2.
10. **Ma Y**, **Liu H**, **Wu J**, **Yuan L**, **Wang Y**, **Du X**, **Wang R**, **Marwa PW**, **Petlulu P**, **Chen X**, **Zhang H.** The adverse health effects of bisphenol A and related toxicity mechanisms. *Environ Res* 176: 108575, 2019. doi:10.1016/j.envres.2019.108575.
11. **Kim MJ**, **Park YJ.** Bisphenols and thyroid hormone. *Endocrinol Metab (Seoul)* 34: 340–348, 2019. doi:10.3803/EnM.2019.34.4.340.
12. **Nadal A**, **Alonso-Magdalena P**, **Soriano S**, **Quesada I**, **Ropero AB.** The pancreatic beta-cell as a target of estrogens and xenoestrogens: implications for blood glucose homeostasis and diabetes. *Mol Cell Endocrinol* 304: 63–68, 2009. doi:10.1016/j.mce.2009.02.016.
13. **Ermini L**, **Nuzzo AM**, **Ietta F**, **Romagnoli R**, **Moretti L**, **Masturzo B**, **Paulesu L**, **Rolfo A.** Placental glucose transporters and response to bisphenol A in pregnancies from of normal and overweight mothers. *Int J Mol Sci* 22: 6625, 2021. doi:10.3390/ijms22126625.
14. **Salehpour A**, **Shidfar F**, **Hedayati M**, **Neshatbini Tehrani A**, **Farshad AA**, **Mohammadi S.** Bisphenol A enhances adipogenic signaling pathways in human mesenchymal stem cells. *Genes Environ* 42: 13, 2020. doi:10.1186/s41021-020-00150-6.
15. **Chianese R**, **Troisi J**, **Richards S**, **Scafuro M**, **Fasano S**, **Guida M**, **Pierantoni R**, **Meccariello R.** Bisphenol A in reproduction: epigenetic effects. *Curr Med Chem* 25: 748–770, 2018. doi:10.2174/0929867324666171009121001.
16. **Konieczna A**, **Rutkowska A**, **Rachoń D.** Health risk of exposure to bisphenol A (BPA). *Rocz Panstw Zakl Hig* 66: 5–11, 2015.
17. **Connors LT**, **Zhu HL**, **Gill M**, **Walsh E**, **Singh RD**, **Easson S**, **Ahmed SB**, **Habibi HR**, **Cole WC**, **Thompson JA.** Prenatal exposure to a low dose of BPS causes sex-dependent alterations to vascular

endothelial function in adult offspring. *Front Toxicol* 4: 933572, 2022. doi:10.3389/ftox.2022.933572.
18. **Negri-Cesi P.** Bisphenol A interaction with brain development and functions. *Dose Response* 13: 1559325815590394, 2015. doi:10.1177/1559325815590394.
19. **Li C**, **Sang C**, **Zhang S**, **Zhang S**, **Gao H.** Effects of bisphenol A and bisphenol analogs on the nervous system. *Chin Med J (Engl)* 136: 295–304, 2023. doi:10.1097/CM9.0000000000002170.
20. **Gerona RR**, **Woodruff TJ**, **Dickenson CA**, **Pan J**, **Schwartz JM**, **Sen S**, **Friesen MW**, **Fujimoto VY**, **Hunt PA.** Bisphenol-A (BPA), BPA glucuronide, and BPA sulfate in midgestation umbilical cord serum in a Northern and Central California population. *Environ Sci Technol* 47: 12477–12485, 2013. doi:10.1021/es402764d.
21. **Atrooz F**, **Alkadhi KA**, **Salim S.** Understanding stress: insights from rodent models. *Curr Res Neurobiol* 2: 100013, 2021. doi:10.1016/j.crneur.2021.100013.
22. **Sarigiannis DA**, **Papaioannou N**, **Handakas E**, **Anesti O**, **Polanska K**, **Hanke W**, **Salifoglou A**, **Gabriel C**, **Karakitsios S.** Neurodevelopmental exposome: the effect of in utero co-exposure to heavy metals and phthalates on child neurodevelopment. *Environ Res* 197: 110949, 2021. doi:10.1016/j.envres.2021.110949.
23. **Gassman NR.** Induction of oxidative stress by bisphenol A and its pleiotropic effects. *Environ Mol Mutagen* 58: 60–71, 2017. doi:10.1002/em.22072.
24. **Gandhi S**, **Abramov AY.** Mechanism of oxidative stress in neurodegeneration. *Oxid Med Cell Longev* 2012: 428010, 2012. doi:10.1155/2012/428010.
25. **Schieber M**, **Chandel NS.** ROS function in redox signaling and oxidative stress. *Curr Biol* 24: R453–R462, 2014. doi:10.1016/j.cub.2014.03.034.
26. **Pangrazzi L**, **Balasco L**, **Bozzi Y.** Oxidative stress and immune system dysfunction in autism spectrum disorders. *Int J Mol Sci* 21: 3293, 2020. doi:10.3390/ijms21093293.
27. **Coussons-Read ME.** Effects of prenatal stress on pregnancy and human development: mechanisms and pathways. *Obstet Med* 6: 52–57, 2013. doi:10.1177/1753495X12473751.
28. **Jin J**, **Menon R.** Placental exosomes: a proxy to understand pregnancy complications. *Am J Reprod Immunol* 79: e12788, 2018. doi:10.1111/aji.12788.
29. **Puttabyatappa M**, **Banker M**, **Zeng L**, **Goodrich JM**, **Domino SE**, **Dolinoy DC**, **Meeker JD**, **Pennathur S**, **Song PXK**, **Padmanabhan V.** Maternal exposure to environmental disruptors and sexually dimorphic changes in maternal and neonatal oxidative stress. *J Clin Endocrinol Metab* 105: 492–505, 2020. doi:10.1210/clinem/dgz063.
30. **Campello E**, **Spiezia L**, **Radu CM**, **Dhima S**, **Visentin S**, **Valle FD**, **Tormene D**, **Woodhams B**, **Cosmi E**, **Simioni P.** Circulating microparticles in umbilical cord blood in normal pregnancy and pregnancy with preeclampsia. *Thromb Res* 136: 427–431, 2015. doi:10.1016/j.thromres.2015.05.029.
31. **Rosenfeld CS.** The placenta-brain-axis. *J Neurosci Res* 99: 271–283, 2021. doi:10.1002/jnr.24603.
32. **Dimasuay KG**, **Boeuf P**, **Powell TL**, **Jansson T.** Placental responses to changes in the maternal environment determine fetal growth. *Front Physiol* 7: 12, 2016. doi:10.3389/fphys.2016.00012.
33. **Caniggia I**, **Mostachfi H**, **Winter J**, **Gassmann M**, **Lye SJ**, **Kuliszewski M**, **Post M.** Hypoxia-inducible factor-1 mediates the biological effects of oxygen on human trophoblast differentiation through TGFbeta(3). *J Clin Invest* 105: 577–587, 2000. doi:10.1172/JCI8316.
34. **Ermini L**, **Farrell A**, **Alahari S**, **Ausman J**, **Park C**, **Sallais J**, **Melland-Smith M**, **Porter T**, **Edson M**, **Nevo O**, **Litvack M**, **Post M**, **Caniggia I.** Ceramide-induced lysosomal biogenesis and exocytosis in early-onset preeclampsia promotes exosomal release of SMPD1 causing endothelial dysfunction. *Front Cell Dev Biol* 9: 652651, 2021. doi:10.3389/fcell.2021.652651.
35. **Welsh JA**, **Goberdhan DCI**, **O'Driscoll L**, **Buzas EI**, **Blenkiron C**, **Bussolati B**, **et al.** Minimal information for studies of extracellular vesicles (MISEV2023): from basic to advanced approaches. *J Extracell Vesicles* 13: e12404, 2024. doi:10.1002/jev2.12404.
36. **Ermini L**, **Mandalà M**, **Cresti L**, **Passaponti S**, **Patrussi L**, **Paulesu L**, **Thornburg K**, **Ietta F.** Fetal myocardial expression of GLUT1: roles of BPA exposure and cord blood exosomes in a rat model. *Cells* 11: 3195, 2022. doi:10.3390/cells11203195.
37. **Livak KJ**, **Schmittgen TD.** Analysis of relative gene expression data using real-time quantitative PCR and the 2(−delta C(T)) method. *Methods* 25: 402–408, 2001. doi:10.1006/meth.2001.1262.
38. **La Rocca C**, **Tait S**, **Guerranti C**, **Busani L**, **Ciardo F**, **Bergamasco B**, **Stecca L**, **Perra G**, **Mancini FR**, **Marci R**, **Bordi G**, **Caserta D**, **Focardi S**, **Moscarini M**, **Mantovani A.** Exposure to endocrine disrupters and nuclear receptor gene expression in infertile and fertile women from different Italian areas. *Int J Environ Res Public Health* 11: 10146–10164, 2014. doi:10.3390/ijerph111010146.
39. **Zorov DB**, **Juhaszova M**, **Sollott SJ.** Mitochondrial reactive oxygen species (ROS) and ROS-induced ROS release. *Physiol Rev* 94: 909–950, 2014. doi:10.1152/physrev.00026.2013.
40. **Narciso L**, **Ietta F**, **Romagnoli R**, **Paulesu L**, **Mantovani A**, **Tait S.** Effects of bisphenol A on endogenous retroviral envelopes expression and trophoblast fusion in BeWo cells. *Reprod Toxicol* 89: 35–44, 2019. doi:10.1016/j.reprotox.2019.07.001.
41. **Blond JL**, **Lavillette D**, **Cheynet V**, **Bouton O**, **Oriol G**, **Chapel-Fernandes S**, **Mandrand B**, **Mallet F**, **Cosset FL.** An envelope glycoprotein of the human endogenous retrovirus HERV-W is expressed in the human placenta and fuses cells expressing the type D mammalian retrovirus receptor. *J Virol* 74: 3321–3329, 2000. doi:10.1128/jvi.74.7.3321-3329.2000.
42. **Sheller-Miller S**, **Radnaa E**, **Arita Y**, **Getahun D**, **Jones RJ**, **Peltier MR**, **Menon R.** Environmental pollutant induced cellular injury is reflected in exosomes from placental explants. *Placenta* 89: 42–49, 2020. doi:10.1016/j.placenta.2019.10.008.
43. **Xia C**, **Dai Z**, **Jin Y**, **Chen P.** Emerging antioxidant paradigm of mesenchymal stem cell-derived exosome therapy. *Front Endocrinol (Lausanne)* 12: 727272, 2021. doi:10.3389/fendo.2021.727272.
44. **Vargas A**, **Zhou S**, **Éthier-Chiasson M**, **Flipo D**, **Lafond J**, **Gilbert C**, **Barbeau B.** Syncytin proteins incorporated in placenta exosomes are important for cell uptake and show variation in abundance in serum exosomes from patients with preeclampsia. *FASEB J* 28: 3703–3719, 2014. doi:10.1096/fj.13-239053.
45. **Circu ML**, **Aw TY.** Reactive oxygen species, cellular redox systems, and apoptosis. *Free Radic Biol Med* 48: 749–762, 2010. doi:10.1016/j.freeradbiomed.2009.12.022.
46. **Cimino F**, **Esposito F**, **Ammendola R**, **Russo T.** Gene regulation by reactive oxygen species. *Curr Top Cell Regul* 35: 123–148, 1997. doi:10.1016/s0070-2137(97)80005-2.
47. **Kakizawa S**, **Arasaki T**, **Yoshida A**, **Sato A**, **Takino Y**, **Ishigami A**, **Akaike T**, **Yanai S**, **Endo S.** Essential role of ROS – 8-nitro-cGMP signaling in long-term memory of motor learning and cerebellar synaptic plasticity. *Redox Biol* 70: 103053, 2024. doi:10.1016/j.redox.2024.103053.
48. **Banks WA**, **Sharma P**, **Bullock KM**, **Hansen KM**, **Ludwig N**, **Whiteside TL.** Transport of extracellular vesicles across the blood-brain barrier: brain pharmacokinetics and effects of inflammation. *Int J Mol Sci* 21: 4407, 2020. doi:10.3390/ijms21124407.